

Transverse Waves in a Two-Dimensional Screened-Coulomb Crystal (Dusty Plasma)

S. Nunomura,* D. Samsonov,† and J. Goree‡

Department of Physics and Astronomy, The University of Iowa, Iowa City, Iowa 52242

(Received 23 February 2000)

Transverse shear waves were observed experimentally in a two-dimensional screened Coulomb crystal. They were excited by applying a chopped laser beam to a 2D dusty plasma, i.e., a monolayer of charged microspheres levitated in a plasma. Measurements of the dispersion relation reveal an acoustic, i.e., nondispersive, character over the entire range of wave numbers measured, $0.2 < k_r a / \pi < 0.7$, where a is the interparticle spacing. Comparison to theory provides a measurement of the particles' charge.

PACS numbers: 52.25.Zb, 52.25.Ub, 52.35.-g, 82.70.Dd

In a screened Coulomb system, charged particles interact through a shielded repulsive Coulomb potential. For a point particle of charge Q , this is the Yukawa potential, $V(r) = Q/4\pi\epsilon_0 r \exp(-r/\lambda_D)$, where r is the distance between two particles and λ_D is the Debye screening length. When it is in thermodynamic equilibrium, the system is characterized by two dimensionless parameters: the ratio of interparticle spacing to shielding length, $\kappa = a/\lambda_D$, and the Coulomb coupling energy normalized by the thermal energy of particles, $\Gamma = Q^2/4\pi\epsilon_0 a k_B T$. When $\Gamma > 1$, the system is said to be strongly coupled.

We will consider waves in a 2D system consisting of a monolayer of charged particles. This system can sustain longitudinal waves and two kinds of transverse waves, where the latter can be classified according to whether particle motion remains *in plane* or is *out of plane*. Here we report experiments with the transverse shear wave, where the particles remain in the monolayer. This mode can propagate a long distance only in a solid medium. It also exists in 3D systems [1,2]. In seismology, it is termed the shear or S wave.

Peeters and Wu presented a phonon spectrum, i.e., a dispersion relation, for a 2D hexagonal crystal with a Yukawa potential [3]. They carried out a numerical calculation of the dynamical matrix of the system, which ignores kinetic effects such as thermal motion and damping. Their motivation was a study of colloidal crystals, although the theory is more broadly applicable.

Our experimental system was a monolayer suspension of charged microspheres, levitated in a plasma. This system is termed a dusty plasma. Because it is analogous to a colloidal suspension, which belongs to the field of complex fluids, a dusty plasma is sometimes called a complex plasma [4]. Electrons and ions serve the dual roles of providing Debye shielding and sustaining a large negative charge Q on the particles. Neutral gas in the plasma cools the particles so that they can become strongly coupled and arrange in a Wigner lattice, sometimes called a plasma crystal [5–8]. In plasma crystal experiments, the particle positions and velocities can be measured precisely, but direct measurements of λ_D and Q are often less precise. The entire system is not in thermodynamic equilibrium, because the particles have a much lower kinetic temperature

than the electrons, and constant energy input is required to sustain the plasma. Nevertheless, the monolayer particle system, by itself, is in an equilibrium that can be characterized by κ and Γ . Konopka's experiments demonstrated that the Yukawa potential is accurate for a single pair of particles moving in a horizontal plane, in an apparatus like ours [9].

Most studies of wave motion in dusty plasmas have dealt with the longitudinal mode. In a 2D suspension, longitudinal waves were observed in a strongly coupled regime [4,10–14], while in 3D they were detected in a weakly coupled regime [15]. In 2D, a possible indication of out-of-plane transverse waves was observed in an experiment where there were spontaneous *out-of-plane* oscillations [16].

In order to excite transverse waves with *in-plane* motion, we used the apparatus [14] shown in Fig. 1. A plasma was produced by an rf voltage between a horizontal electrode and the surrounding vacuum chamber, which acted as ground. The voltage was 49 V (peak to peak) at 13.6 MHz, with no measurable dc bias. The gas was room-temperature argon at 5 mtorr. To characterize the main plasma region, located above the particle monolayer, we used a Langmuir probe. The plasma potential was 35.8 V with respect to ground. The electrons had a temperature $T_e \approx 2.1$ eV and density $n_e \approx 6 \times 10^8$ cm $^{-3}$, corresponding to $\lambda_D \approx 440$ μ m. In the sheath region, where the microspheres were located, the plasma density is

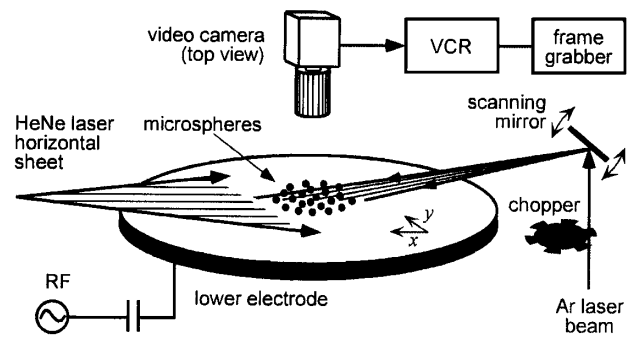


FIG. 1. Sketch of experimental apparatus. A modulated laser sheet excites transverse waves in a plasma crystal. Charged microspheres are levitated above a horizontal electrode.

reduced. In that region we will assume that $\lambda_D > 570 \mu\text{m}$. These parameters, based on Langmuir probe measurements in the main plasma, have an accuracy of perhaps a factor of 2.

The particles were polymer spheres, $6.5 \mu\text{m}$ in diameter with $\pm 0.3 \mu\text{m}$ size dispersion and a density of 1.51 g/cm^3 . They fell into the plasma and settled in a monolayer, where they were levitated by an electric field in the sheath region above the electrode. They formed a triangular lattice with hexagonal symmetry. The inter-particle spacing was measured precisely, as the first peak of the pair correlation function $g(r)$, to be $a = 825 \mu\text{m}$. Accordingly, we estimate that $\kappa < 1.4$. Using structural analysis methods [17], the translation correlation length and the orientation correlation length were found to be $21a$ and $75a$, respectively. These large values indicate a highly ordered lattice. One of the primitive translation vectors of the lattice was in the y direction.

Particles were trapped in the vertical direction by a combination of gravity and the sheath electric field. This trapping did not allow any measurable *out-of-plane* motion during the experiment. A gentle bowl-shaped curvature in the sheath provided radial confinement.

Waves were excited by a laser's radiation pressure. In this scheme, developed originally by Homann [11] for launching longitudinal waves, an argon laser is chopped mechanically. Here we expanded the beam into a horizontal sheet by using a scanning mirror. The laser sheet was then incident on the crystal at a grazing angle of $\approx 10^\circ$, so that it applied a force mainly in the $+x$ direction [14]. The region that was irradiated was a narrow stripe, extending across the entire lattice in the x direction. In the y direction it had a Gaussian profile with a FWHM of 0.5 mm . The 300 Hz frequency of the scanning mirror was much higher than any waves that propagate in the lattice, so that for practical purposes particles in the irradiated region experienced a constant force, except when the laser was blocked by the chopper.

To image the particles, we illuminated them with a horizontal laser sheet, and viewed them with a video camera through the top window. The camera was operated at 30 frames/s . It had a field of view of $24 \times 18 \text{ mm}$, which included 740 particles. The images were digitized with an 8-bit gray scale and 640×480 pixel resolution. The x - y coordinates of particles were measured with sub-pixel resolution in each frame, and individual particles were traced from one frame to the next, using the method of Refs. [4,13,14]. The time series was 128 frames, corresponding to 4.27 s .

We performed two kinds of transverse shear wave experiments. First, we observed the propagation of a single pulse excited by a pulse of 600 mW laser light. Second, we observed sinusoidal wave propagation by chopping the laser with a 50% duty cycle, operating at 200 mW .

The pulse propagation experiment clearly illustrates how particles move transverse to the direction of wave propa-

gation. Figure 2(a) shows velocity maps of particles in the crystal. Initially, during the 0.33 s laser pulse, particles in the excitation region were pushed in the $+x$ direction by the radiation pressure. Later, the particle motion was still in the $+x$ direction, but it was localized in a pulse that had moved away from the excitation region in the y direction. Because the pulse propagates at 90° compared with the particle motion, the wave has a shear or transverse character.

The same data are shown as a smoothed profile in Fig. 2(b), revealing the propagation speed of the wave. Plotted here is v_x vs y , where we have averaged v_x over the ignorable coordinate x . In these plots the most prominent feature is the pulse of forward particle motion, $v_x > 0$. The restoring motion, $v_x < 0$, is slower; it can be seen near $y = 0$ and $t = 0.7 \text{ s}$. The curves in Fig. 2(b) are displaced by a constant time interval, so that drawing a line through their peaks gives the propagation speed. The pulse propagation speed, $6.1 \pm 0.5 \text{ mm/s}$, is very slow. Indeed, among plasma waves, it is the slowest of any kind known

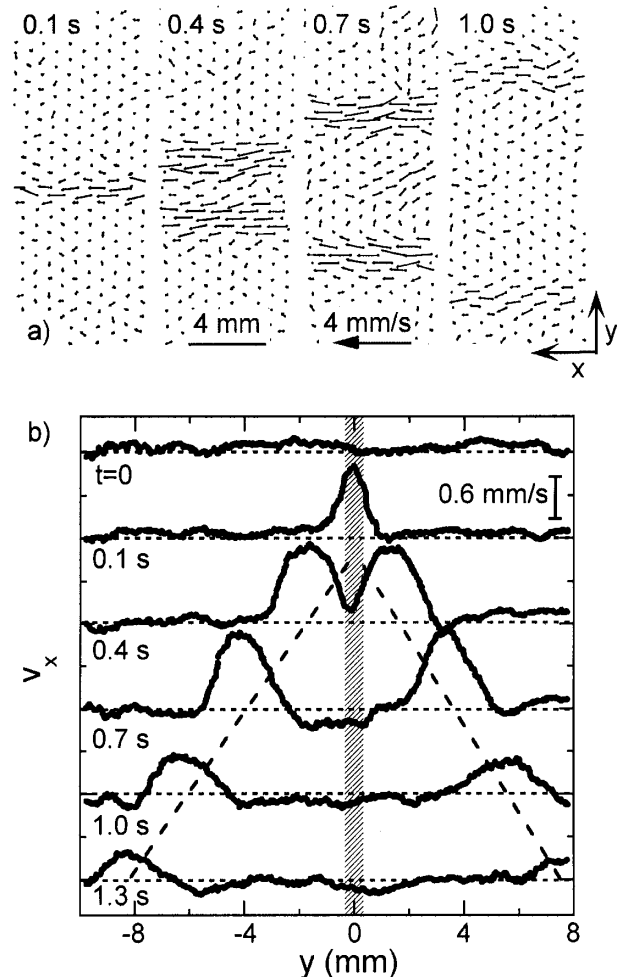


FIG. 2. Pulse propagation. (a) Velocity map of particles. (b) Profile of v_x . The excitation region, shown shaded, is irradiated by the laser.

to the authors. Nevertheless, the particle motion in the x direction is even slower, ~ 1 mm/s.

Next, we present experimental results for the periodic wave. The waveform of the laser is a square wave, which has harmonics. However, the particle motion associated with harmonics was weak, as we will show, and will be eliminated by using a Fourier transform technique.

To illustrate the wave's oscillation, we show in Fig. 3(a) a profile of v_x vs y , for a fundamental driving frequency $\omega/2\pi = 2.0$ Hz. This is like Fig. 2(b), except that the excitation is periodic rather than pulsed. The shear motion is almost sinusoidal, with a wavelength ≈ 3.0 mm in the transverse direction. Note that the particles oscillate in both the $+x$ and $-x$ directions, even far from the excitation region. Note also that as the wave becomes gradually weaker it propagates away from its source; this is attributed to damping on the gas, as we will explain below.

The low amplitude of the particle motion suggests that the wave motion is linear. The amplitude was approximately 0.2 mm/s and $0.06a$, for velocity and position, respectively. A peak at the second harmonic, which would be a signature of nonlinear harmonics generation, is absent from our spectrum in Fig. 3(b). We note that the third harmonic has a peak weaker than $\frac{1}{3}$ the fundamental peak, as would be expected for a square wave, perhaps due to a stronger wave damping at higher ω .

As a test, we checked for modulation of the number density, which would reveal the presence of any longitudinal waves. To do this, we used the density-mapping method of Ref. [4]. We found that any such modulation was weaker than our 3% detection limit.

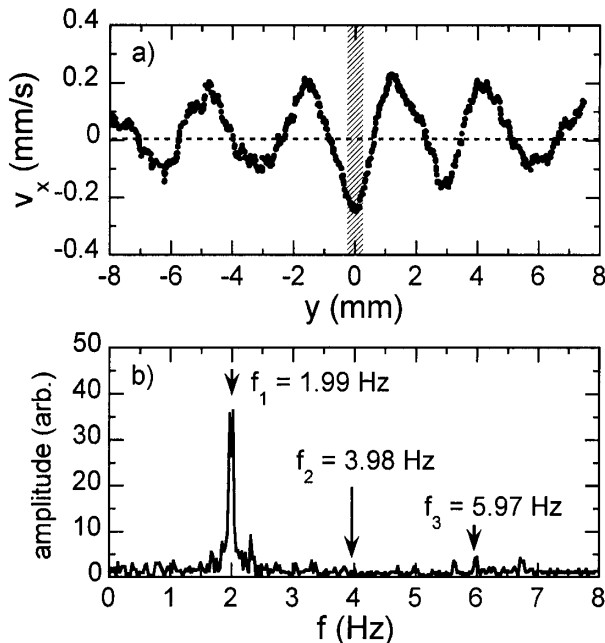


FIG. 3. Periodic waves. (a) Profile of v_x for a periodic wave at a chopping frequency $\omega/2\pi = 2$ Hz. (b) Wave spectrum in the excitation region.

Our chief results are a measurement of the wave number $k = k_r + ik_i$, made using a temporal Fourier transform of the particle motion associated with the fundamental frequency ω . The y dependence of phase and amplitude were fit to a line and an exponential decay, respectively, yielding k_r and k_i . We used the method of Ref. [10], except that we chose v_x rather than x as the input data, thereby reducing the method's sensitivity to secular particle drift.

The experimentally measured dispersion relation, Fig. 4(a), exhibits an acousticlike relation, $\omega \propto k_r$. In other words, the wave is a nondispersive sound wave. This is true over the range of wave numbers we measured, from $k_r a/\pi = 0.2$ to 0.7 . The sound speed of the transverse wave, i.e., the slope of ω vs k , is $C_t = 6.7 \pm 0.5$ mm/s. This result is consistent with the pulse speed reported above. The pulse was excited by a higher power, and it was otherwise produced under the same conditions.

The damping of the wave, as indicated by k_i , was weak, due to the low gas pressure. In Fig. 4(a), $k_i a/\pi$ ranged

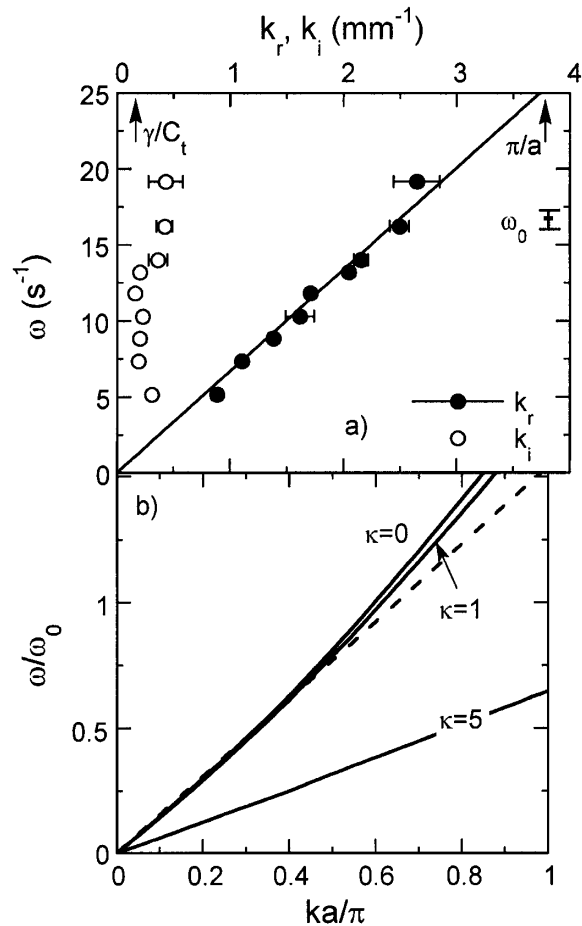


FIG. 4. Dispersion relation. (a) Experimentally measured k_r and k_i are shown as filled and open circles, respectively. A solid line indicates the sound velocity C_t . (b) Phonon spectrum of Peeters and Wu [3]. The broken line was calculated for $\kappa = 1$ from Eq. (1).

from 0.042 to 0.11, with the strongest damping at the highest frequencies. This is comparable to a simple estimate $\gamma/C_t = 0.047$, based on the Epstein drag coefficient γ for molecular gas collisions with a sphere [18]. The damping time, $\gamma^{-1} = 0.82$ s, was much longer than for a colloidal suspension.

We now compare the experimental dispersion relation to the phonon spectrum of Peeters and Wu [3]. Their triangular lattice with a Yukawa potential resembles our experiment, except that it neglects damping, thermal effects, and deviations from perfect translation and orientational order. Assuming the model is correct, we will use it to calculate Q in the experiment, and from that we estimate the quantities Γ and Einstein frequency ω_E .

The model has a linear relationship $\omega \propto k_r$ for small wave numbers, $k_r a/\pi < 0.5$, as shown in Fig. 4(b). For larger wave numbers, it begins to curve, although the curvature is weak for the $k_r a/\pi < 1$ range where the experiment was performed. A broken line in Fig. 4(b) shows an extrapolation of the $\kappa = 1$ curve for small k_r . According to the model, the transverse sound C_t is almost independent of κ for small κ ; it varies only 20% over the range $0 < \kappa < 2$. Peeters and Wu fit their numerical results for small κ and small k_r , and found

$$C_t/C_0 = 0.51317 - 0.0226(\kappa/1.0745699)^2, \quad (1)$$

where $C_0^2 \equiv \omega_0^2 a^2 \equiv Q^2/4\pi\epsilon_0 m a$, m is the particle mass, and ω_0 is analogous to a plasma frequency.

Using Eq. (1) with the experimentally measured C_t , we find that Q/e is in the range $-11\,500$ to $-12\,500$, for $\kappa = 0$ and 1.4, respectively. Hereafter we will assume a value in the middle of this range, $Q/e = -12\,000$. This result is based on experimental measurements of C_t and a , which are precise, our estimate $\kappa < 1.4$, which is less precise, and the assumption that the Peeters and Wu model is valid.

The curves in Fig. 4 are normalized by ω_0 . Using $Q/e = -12\,000$ along with our precisely measured value of a , we find $\omega_0 = 16.6 \pm 0.7$ s⁻¹ for the experiment.

In comparing experiment and theory in Fig. 4, it is significant that $\omega \propto k_r$ in both dispersion relations, over the range of wave numbers shown. This is one of our chief results. It is not significant, however, that ω/ω_0 vs k_r has the same slope in both cases. That is because, as described above, we chose Q and therefore ω_0 so that the experimental C_t agrees with the theory.

The Einstein frequency, a characteristic frequency of a crystal, is defined as $\omega_E^2 = Qm^{-1} \sum \partial^2 V(r)/\partial r^2$, summed over six interparticle bonds. For $Q/e = -12\,000$, we calculate $\omega_E = 29.9 \pm 1.7$ s⁻¹ for $0 < \kappa < 1.4$.

The Coulomb coupling parameter is calculated from the particle kinetic temperature, which we measured to be 0.048 eV by fitting the particle velocity distribution to a Gaussian. Therefore, Γ is estimated to be about 5300, and $\Gamma \exp(-\kappa)$ is smaller than this by a factor of 2. The high value of Γ indicates that the system is strongly coupled, in agreement with our observation of a highly ordered hexagonal lattice.

In summary, we excited transverse shear waves in 2D screened Coulomb crystal by applying radiation pressure to a dusty plasma. The experimentally measured dispersion relation has a nondispersive characteristic over a wide range of k_r . Assuming the Peeters and Wu model [3] is correct, we calculated Q from the measured sound speed C_t . The accuracy of this method of measuring Q requires tests that are planned for a future experiment.

We thank X. Wang, Z. W. Ma, A. Bhattacharjee, and R. A. Quinn for valuable discussions and F. M. Peeters and A. Sen for useful communications. The work was supported by NASA and the National Science Foundation. S. N. was supported by the Japan Society for the Promotion of Science.

*Electronic address:

†Current address: Max-Planck-Institut für Extraterrestrische Physik, Giessenbachstrasse, 85740 Garching, Germany.

‡Electronic address:

- [1] P. K. Kaw and A. Sen, Phys. Plasmas **5**, 3552 (1998).
- [2] X. Wang and A. Bhattacharjee, Phys. Plasmas **6**, 4388 (1999).
- [3] F. M. Peeters and X. G. Wu, Phys. Rev. A **35**, 3109 (1987).
- [4] D. Samsonov, J. Goree, H. M. Thomas, and G. E. Morfill, Phys. Rev. E (to be published).
- [5] J. H. Chu and Lin I, Phys. Rev. Lett. **72**, 4009 (1994).
- [6] H. Thomas *et al.*, Phys. Rev. Lett. **73**, 652 (1994).
- [7] Y. Hayashi and K. Tachibana, Jpn. J. Appl. Phys. **33**, L804 (1994).
- [8] A. Melzer, T. Trottenberg, and A. Piel, Phys. Lett. A **191**, 301 (1994).
- [9] U. Konopka, G. E. Morfill, and L. Ratke, Phys. Rev. Lett. **84**, 891 (2000).
- [10] J. B. Pieper and J. Goree, Phys. Rev. Lett. **77**, 3137 (1996).
- [11] A. Homann, A. Melzer, S. Peters, and A. Piel, Phys. Rev. E **56**, 7138 (1997).
- [12] A. Homann *et al.*, Phys. Lett. A **242**, 173 (1998).
- [13] D. Samsonov *et al.*, Phys. Rev. Lett. **83**, 3649 (1999).
- [14] A. Melzer, S. Nunomura, D. Samsonov, Z. W. Ma, and J. Goree (unpublished).
- [15] A. Barkan, R. L. Merlino, and N. D'Angelo, Phys. Plasmas **2**, 3563 (1995).
- [16] S. Nunomura, T. Misawa, N. Ohno, and S. Takamura, Phys. Rev. Lett. **83**, 1970 (1999).
- [17] R. A. Quinn *et al.*, Phys. Rev. E **53**, R2049 (1996).
- [18] P. Epstein, Phys. Rev. **23**, 710 (1924).